

# An Active Particle-based Tracking Framework for 2D and 3D Time-lapse Microscopy Images

M. Julius Hossain, *Member, IEEE*, Paul F. Whelan, Senior Member, IEEE, Andras Czirok and Ovidiu Ghita

**Abstract**—The process required to track cellular structures is a key task in the study of cell migration. This allows the accurate estimation of motility indicators that help in the understanding of mechanisms behind various biological processes. This paper reports a particle-based fully automatic tracking framework that is able to quantify the motility of living cells in time-lapse images. Contrary to the standard tracking methods based on predefined motion models, in this paper we reformulate the tracking mechanism as a data driven optimization process to remove its reliance on a *priori* motion models. The proposed method has been evaluated on 2D and 3D fluorescence *in-vivo* image sequences that describe the development of the quail embryo.

## I. INTRODUCTION

THE study of cell migration is of a great significance in various fields of research including embryonic development, drug discovery and wound healing [1]-[3]. In the quantification of the cell migration, the accurate tracking of cellular structures is a key task that determines the location and the association rules between the cells throughout the image sequence. With the advent of modern microscopy imaging modalities the volume of image data has vastly increased and as a consequence the manual tracking of individual cell has become tedious and even impossible when dealing with large dense cellular data sets. Also, the variety of cellular imaging techniques, different cell types, changes in cell morphology over time and random motion of the cells raise significant challenges that have to be overcome by the automatic cellular tracking algorithms. As a result, the development of a unique solution that works well on all type of cells and imaging condition is impractical. Thus, the study of cell migration using computer vision based techniques entails a highly collaborative and multi-

disciplinary research [4]. To this end engineering efforts concentrate on the development of tracking solutions, while molecular scientists focus on the investigation of the biological implications associated with motility patterns.

The major challenges associated with automated cell tracking are related to several factors such as the noise inserted in the imaging process, random motion patterns, changes in the appearance of cells over time, deformation, cellular interaction, photo-bleaching, etc. Various methods have been proposed to address the above challenges and they can be broadly classified into two categories [2],[3],[5]. In the first category cells are detected in each frame and the cell to cell correspondence is carried out for each two adjacent frames in the sequence [3],[6]. Methods included in the second category detect cells in the first frame, identify model parameters and perform tracking by evolving the model in subsequent frames. The effectiveness of methods in the first category is largely dependent on the success of segmentation which is problematic when the number of cells is large and they are not well separated. In this regard, to avoid the segmentation of cells in each frame in the process of tracking *in-vivo* cellular data, most of the research efforts have been devoted to the development of model based tracking techniques where the robust identification of the motion patterns represents the major challenge.

Model based techniques based on Kalman and particle based filters estimate the system model parameters to guide the tracking process for each cell in the image sequence [7],[8]. However, due to the self propelled motility of cells, their motion characteristics may not be known in advance to obtain a suitable system model that incorporates all modes of motion. To compensate for this problem, the estimation of the motion patterns has been carried out using multiple statistical models [9]. Although these algorithms include multiple models corresponding to different cellular movement types, they entail a considerable level of supervision that is required to identify the motility patterns. Some methods incorporate the current observation data along with the motion model to obtain better tracking performance [10],[11]. In this regard, several hybrid methods have been reported where a transition model was combined with an independent mean shift algorithm [11],[12]. These methods lead to improvement in tracking accuracy, but they cannot accommodate cell displacements larger than the kernel size.

Manuscript received April 15, 2011. This work was supported through the National Biophotonics and Imaging Platform, Ireland, and funded by the Irish Government's Programme for Research in Third Level Institutions, Cycle 4, Ireland's EU Structural Funds Programmes 2007-2013. Microscopy data was obtained through support of the NIH (R01HL087136, R01HL068855 and R01 HL068855).

M. J. Hossain is with the Centre for Image Processing and Analysis, Dublin City University, Glasnevin, Dublin 9, Ireland (phone: +353-1-700-7637; fax: +353-1-700-5508; e-mail: julius.hossain@dcu.ie).

P. F. Whelan is with the Department of Electronic Engineering, Dublin City University, Glasnevin, Dublin 9, Ireland (e-mail: paul.whelan@dcu.ie)

A. Czirok is with the Department of Anatomy and Cell Biology, Kansas University Medical Centre, KS 66160, USA (e-mail: aczirok@kumc.edu).

O. Ghita is with the Centre for Image Processing and Analysis, Dublin City University, Glasnevin, Dublin 9, Ireland (e-mail: ghita@eeng.dcu.ie).

The analysis of 3D motion is becoming increasingly important in the studies that address the molecular and cellular domain, but so far only a limited number of papers have been reported on 3D cell migration [12]-[13]. Most of the existing methods that address the 3D cell motion rely on the use of projected 2D data. Thus, the motility information obtained through this 3D to 2D projection process cannot precisely describe the 3D cell migration. For instance in 3D, when one cell passes above or beneath another, the motion is perceived as penetration or merging in the projected 2D data. As a result, in this situation the cell tracking using projected data will return an inaccurate estimation of the real 3D cell motion.

In this paper we proposed a novel tracking framework that is able to extract motility information on both 2D and 3D in-vivo cellular data. The proposed method does not require prior knowledge about the motion model or assumptions in regard to the image noise. Here the target is represented by a set of active particles and tracking is performed by evolving these particles into subsequent frames. The particle tracking process in the proposed method is data-driven where the level of similarity between the target candidate and the target model is evaluated in an adaptive framework to minimize the occurrence of incorrect tracking decisions. To track cells in 3D within a series of image stacks, in addition to in-plane searches, the algorithm evaluates the data in adjacent optical planes to infer the cell motion along the  $z$ -axis.

## II. OVERVIEW OF THE PROPOSED FRAMEWORK

The first step of the proposed tracking framework involves cell detection which is a data dependent process. In the proposed framework the cellular structures are automatically detected (full details about this process is provided in Section IV) where a set of particles is employed to sample the area around the centroid of each of the detected cells. Then, particles are propagated in the next frame based on the displacement that is estimated for each cell using the Newton Raphson iterative minimization with a pyramidal image decomposition. The minimization procedure is carried out starting from the image with the lowest resolution towards the image with the highest resolution in the pyramidal image decomposition. Once the displacement of a particle is determined, the likelihood is estimated using the intensity distribution calculated within the window  $W$  in two successive frames. A penalty measure is calculated for each particle in agreement to the distance transformed image to prevent incorrect cellular associations when multiple cells are spatially close. A cell is localized in next frame based on the likelihood and penalty score associated with all the particles that have been employed to represent the cell.

When the algorithm is applied to 3D data, in order to address the cell motion along the  $z$ -axis two adjacent optical planes immediately above and below the plane under evaluation are also analyzed. The plane that has the highest likelihood is selected as the target location for next frame. It

is useful to note here that in 3D stack images the spatial resolution along the  $z$ -axis is much lower than that along  $xy$ -plane. The datasets used in our experiments have only 7 to 9 planes in the  $z$ -axis, where an individual nucleus is fully visible at most in two adjacent planes.

## III. THE PROPOSED METHOD

To implement the cellular tracking, the proposed method propagates the particles associated with the cell in the frame under investigation to the next frame based on the image information without any knowledge about *a priori* motion model. Since it is not possible to determine the location of a particle in the subsequent frame based only on the information of a single pixel, a small window centered on the pixels of interest is used. In our approach, the objective is to determine the displacement  $d$  of a feature calculated within the window  $W$  from frame  $F^T$  to the next frame  $F^{T+1}$  by minimizing the error,

$$e = \int_{s \in W} h(s) [I^{T+1}(s+d) - I^T(s)]^2 ds. \quad (1)$$

where,  $h$  is a weighting function,  $I^T(s)$  represents the intensity value of  $F^T$  at  $s$  and  $T$  defines the time index. The estimation of  $d$  can be formulated as a standard optimization problem. Several techniques have been proposed in the literature to minimize  $e$  in (1) and the most common include the steepest descent, conjugate gradient and Newton-Raphson minimization. When  $d$  is small, the Newton-Raphson minimization has been proved to be the most efficient approach [14],[15] and it has been also employed in our implementation. In relation to (1) we define  $h$  as a Gaussian kernel to emphasize the central area of the window.

$$h(r) = \begin{cases} 1-r^2, & r < 1 \\ 0, & \text{Otherwise} \end{cases}. \quad (2)$$

where  $r$  is the distance from the center of the window. In our algorithm, the size of the window is odd i.e.  $W = (2w+1) \times (2w+1)$  where  $w$  is the half window width. The displacement  $d$  is solved using the following equation,

$$Gd = e. \quad (3)$$

where  $G = \int_{s \in W} g(s)g(s)^T ds$  is a  $2 \times 2$  coefficient matrix which is computed by estimating gradients and their second order moments, and  $e$  is estimated using (1). Here,  $d$  is assumed to be constant within the window and the optimum solution is obtained by applying the Newton-Raphson minimization. In our implementation to accommodate large motion, a multi-resolution image pyramid is created where the number of pyramid levels  $n$  is dynamically determined based on  $w$  and the maximum instantaneous cell migration. Let  $s$  be the location associated with a particle. The corresponding location  $s_L$  in a pyramid level  $L$  is computed

as follows,

$$s_L = s / 2^L. \quad (4)$$

where,  $L \in [0, n-1]$ . Within this framework, features are tracked from the coarsest to the finest resolution, i.e. the result at each resolution provides the initial solution to be analyzed at the subsequent resolution. Thus, the proposed framework is able to deal with large displacements at the top of the pyramid, while maintaining sub-pixel accuracy at the bottom. Using this approach, the particle tracking process is guided based on image properties rather than using *a-priori* defined motion models.

Once a particle is tracked, i.e. the value of  $d$  is determined, the similarity between two corresponding windows is estimated by using an intensity histogram due to its independence to scaling and rotation [10][16]. In this process, the weighting function  $h$  is used to emphasize more the image data close to the central region of the window. We denote  $b(s) \in \{1, 2, \dots, m\}$  as the bin index of the intensity signal at  $s$  where  $m$  denotes the number of bins. The intensity distribution at  $s$  is determined as follows,

$$\{p_s^{(u)}\}_{u \in [1, m]} = K \sum_{s_j \in W} w \left( \frac{|s - s_j|}{\sqrt{2}|W|} \right) \delta[b(s_j) - u]. \quad (5)$$

where,  $\delta[\cdot]$  is the Kronecker delta function,  $K$  is a normalization constant ensuring  $\sum_{i=1}^m p_s^{(u)} = 1$ ,  $|W|$  is the size of the feature window. The distribution calculated with equation (5) assigns a probability for each of the  $m$  bins. The likelihood between distribution  $p_s$  and its corresponding distribution  $p_{s+d}$  is computed as follows,

$$L[p_s, p_{s+d}] = e^{-D[p_s, p_{s+d}]}. \quad (6)$$

where,  $D[p_s, p_{s+d}]$  is the Hellinger distance calculated using equation (7). As, the likelihood of a distribution  $p_s$  is always calculated with respect to its corresponding distribution  $p_{s+d}$ , it is simply denoted by  $L[p_s]$ .

$$D[p_s, p_{s+d}] = \sqrt{1 - \sum_{u=1}^m \sqrt{p_s^{(u)} p_{s+d}^{(u)}}}. \quad (7)$$

Due to the unconstrained motion, cells may come close to each other or interact. This situation leads to incorrect tracking decisions when multiple cells in a frame tend to match with a particular cell in the next frame. To deal with this problem, we calculate a penalty force  $E[x^i]$  associated with each particle  $x^i$  based on its distance with respect to other targets being tracked. Let  $s^i$  be the location of a particle  $x^i$  that is associated with the  $r^{\text{th}}$  target  $o_r$ . Now, the

penalty force associated with  $x^i$  is defined as,

$$E[x^i] = e^{-\min_{t \in [1, M]} \text{dis}(s^i, s_t)}, \quad t \neq r. \quad (8)$$

where,  $s_t$  represents the centroid of a target  $o_t$ ,  $\text{dis}(s^i, s_t)$  represents the  $L_2$  distance between  $s^i$  and  $s_t$ ,  $M$  is the total number of objects being tracked. Thus, to determine the penalty measure associated with a particle, (8) evaluates its distance with respect to the other objects being tracked. It assigns a higher penalty force to the particle having objects in closer neighborhood. To reduce the computational time required to determine the pair-wise distances in (8), a two-pass algorithm based on the Chamfer 5/7 distance has been used [17]. It would be useful to note that the penalty measure in (8) is dependent on the local neighborhood around each particle, hence it models the cellular interactions more accurately than the object-wise repulsive force assignment based on Markov random field [18]. To achieve a better localization, the state of an object  $o_r$  is determined based on the likelihood and penalty force of the particles associated with it.

$$x_r = \sum_{i=1}^{N_r} x^i \times \frac{L[x^i]}{\beta_r \times E[x^i]}, \quad r \in [1, M]. \quad (9)$$

where, particle  $x^i$  is associated with target  $o_r$ ,  $N_r$  is the number of particles that have been used to represent  $o_r$  and  $\beta_r$  is a normalization factor that is computed as follows,

$$\beta_r = \sum_{i=1}^{N_r} \frac{L[x^i]}{E[x^i]}. \quad (10)$$

Thus, the likelihood function is computed based on the similarity between two corresponding regions where the correspondence is represented by the vector  $d$  which is determined using a data-driven optimization process. It would be useful to note here that equation (9) is used to track cell migration in 2D.

To track cell nuclei in 3D within a series of image stacks, the proposed method additionally searches two adjacent optical planes immediately above and below the plane of interest and determines the likelihood. Let  $z$  be the index of current optical plane. So, to track a target  $o_r \in F_z^T$  the proposed method analyzes three frames  $F_{z-1}^{T+1}$ ,  $F_z^{T+1}$  and  $F_{z+1}^{T+1}$ . Here,  $F_z^T$  represents the frame in plane  $z$  at time  $T$ . Let  $C_{r,k}$  be the matching confidence of object  $o_r$  in plane  $k$ , which is computed as follows:

$$C_{r,k} = \sum_{i=1}^{N_r} \frac{L_k[x^i]}{\beta_r \times E_k[x^i]}. \quad (11)$$

where  $L_k$  and  $E_k$  are the likelihood and the penalty measure that are calculated when  $F_k^{T+1}$  is analyzed. The plane which

provides the highest matching confidence is selected as the new  $z$ -coordinate of  $o_r$ ,

$$\hat{z} = \arg \max_{k \in [z-1, z+1]} C_{r,k}. \quad (12)$$

#### IV. EXPERIMENTS AND RESULTS

The proposed tracking framework has been evaluated on both 2D and 3D time-lapse cellular image sequences. The experimental tests have been performed on a large number of deconvolved (Autoquant X, Media Cybernetics, Bethesda, MD, USA) time-lapse florescent microscopy image sequences that record the in-vivo development of transgenic quail embryos. In these embryos the nuclei of the endothelial (vascular) cells are labeled with a GFP (green fluorescent protein) variant [19]. Images are captured in multiple adjacent fields and optical planes using a wide-field epifluorescence microscope [20] with an  $xy$  resolution of 1.3  $\mu\text{m}/\text{pixel}$  and the time interval between two frames is ranging between 4 to 8 minutes. The number of optical ( $z$ ) planes varies from 7 to 9 and the distance between two consecutive planes is 42  $\mu\text{m}$ . Fluorescence intensities are projected onto a single plane where color-coding indicates their origin in the various optical sections. The resulting color coded image sequence is used for the cell tracking procedure. Fig. 1(a) shows the DIC image of a quail embryo where a region of interest (ROI) for cellular tracking is marked with a red rectangle. Fig. 1(b) illustrates the corresponding florescent image of the segment marked with the rectangle in Fig. 1(a). Fig. 1(c) shows an image stack of 5 optical planes where an individual nucleus is clearly visible in two consecutive planes and it is not prominent in other planes. Thus, to track a cell migration along  $z$ -axis, the proposed method probes the current plane and the two immediately adjacent planes.

Cells are automatically detected using a multi-stage segmentation approach. In the initial stage, an image sharpening operation is performed on the intensity data to highlight the inner region of the nuclei. Next, a given number of cells (user defined) are detected progressively based on the strength of the peaks in the intensity sharpened data and a minimum distance among the cells is enforced during this process to achieve a better distribution of the detected cells within the image data domain. To enforce a minimum distance between cells, once a cell is detected the surrounding area within the given distance is marked to disregard the potential peak on that region. In proposed method, the cell detection process evaluates the relative intensity difference between the foreground (cellular structures) and background information, thus it can be used in different imaging condition without resorting to arbitrary thresholds. To detect cell nuclei in a 3D image stack, all the  $z$  planes are taken into consideration while selecting the given number cells. Thus, the number of detected cells in a particular plane might be quite different from that detected in other planes.

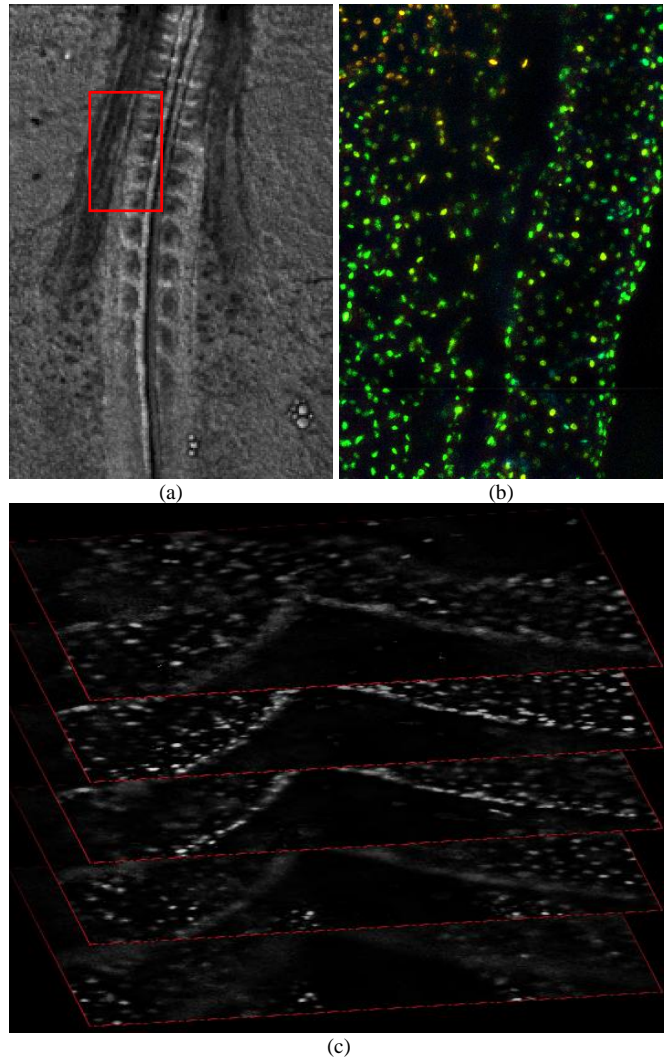


Fig. 1. Sample microscopy images (a) DIC image of a quail embryo. (b) The fluorescence image of the segment marked by the rectangle in Fig. 1(a). (c) Five optical planes. (This diagram is best viewed in color)

To extract the motility information in 2D, the proposed method is applied on several quail sequences where the number of frames in a sequence varies between 87 and 160. We used a  $9 \times 9$  feature window where the maximum expected cell displacement between two consecutive frames is 15 pixels. Fig. 2 shows the visual tracking results obtained when the algorithm is applied to *in-vivo* quail embryo data. Fig. 2(a) and 2(b) show the result where 100 and 200 cells, respectively, have been detected in the first image where Fig. 2(b) includes 100 new cells in addition to the cells that are present in Fig. 2(a). Lineages of the tracked cells in Frames 80 and 87 are shown in Figs. 2(c) and 2(d), respectively. Fig. 2(e) shows the color coded trajectories of the tracked cells in Frame 87 where red and blue denote initial position and final position, respectively. These trajectories indicate the formation of a well-defined crescent-shaped field from which future endocardial cells are recruited. Their dynamics can be validated using the corresponding DIC images shown in Fig. 2(f) where the arrow indicates the direction of the cell migration during the heart development process.

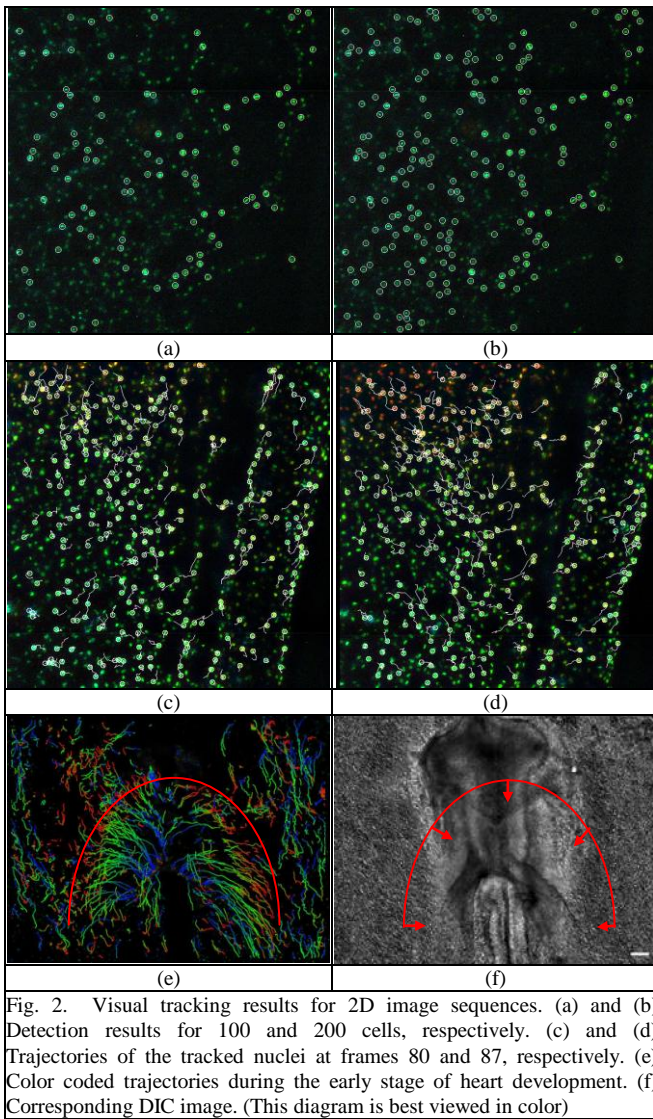


Fig. 2. Visual tracking results for 2D image sequences. (a) and (b) Detection results for 100 and 200 cells, respectively. (c) and (d) Trajectories of the tracked nuclei at frames 80 and 87, respectively. (e) Color coded trajectories during the early stage of heart development. (f) Corresponding DIC image. (This diagram is best viewed in color)

Fig. 3 illustrates the tracking results in 3D for a series of image stacks. Fig. 3(a) shows the detection results for 200 cells where a different color is used to mark the cells in each plane. For clarity purposes, the 3D trajectories are displayed in two forms. In Fig. 3(b) the color coded trajectories are overlaid on the maximum intensity projected image. In this diagram, the movement along the z axis is indicated by the change in the color of the trajectory with respect to the color associated with the plane it moves into. In Figs. 3(c) and 3(d) the direction of the nuclei movements within the 3D volume is illustrated from two different directions.

The tracking process records the locations of the cells in each frame that are used to calculate different motility statistics including instantaneous velocity, distance-traveled, cellular-cycle, motion directionality, etc. These statistics are useful in the analysis of the key processes in different stages of the embryonic development. Fig. 4 depicts the normalized instantaneous velocities of the cells in different stages of the heart development. This diagram shows a reduction in the growth rate of the heart development at the later stages of the organ formation.

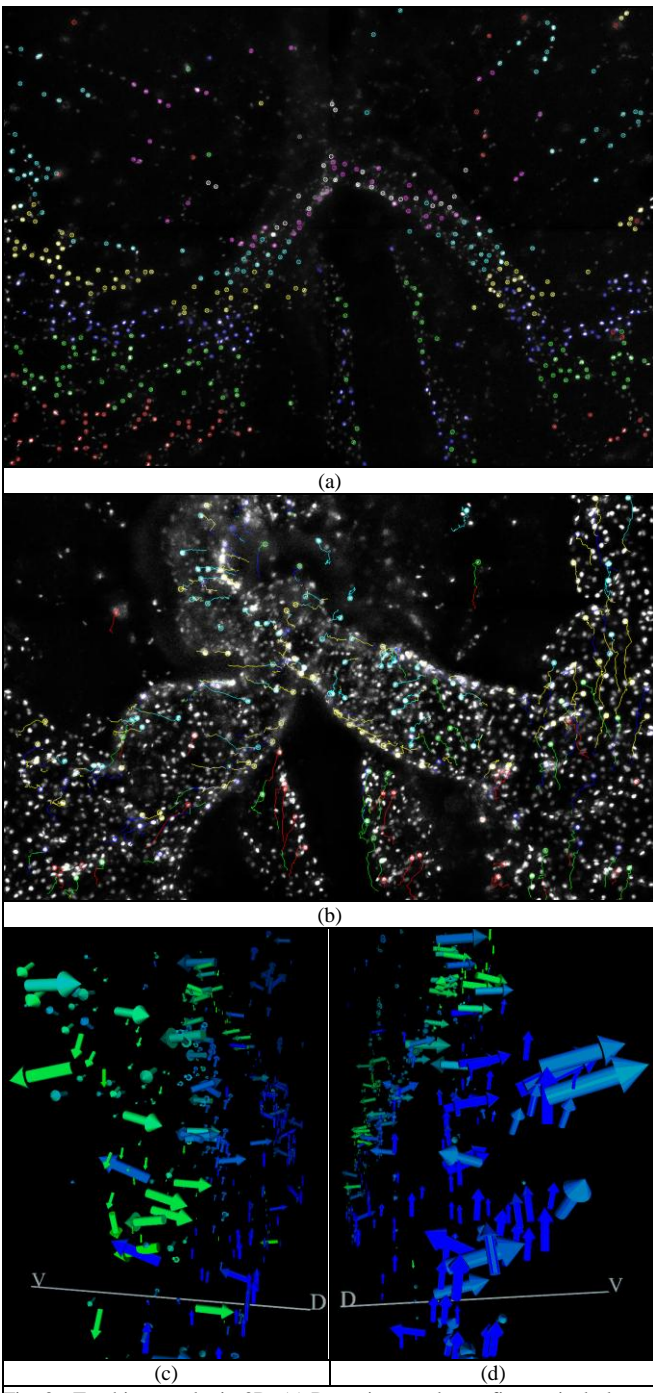


Fig. 3. Tracking results in 3D. (a) Detection results on five optical planes. (b) Trajectories of tracked cells in maximum intensity projected image. (c) and (d) Direction of cell motion in a 3D volume viewed from two different directions. (This diagram is best viewed in color)

As discussed earlier, the velocity of the cells extracted by the tracking algorithm is one of the key parameters employed to measure the growth rate associated with different organ formation processes. Thus, we evaluated the performance of the developed tracking method in regard to how well it computes the instantaneous cell velocity by comparing its performance with respect to the manually annotated data. The average deviation between the cell velocities that are determined using the manual annotated data and the

proposed method is less than 8%. Fig. 5 shows the velocity normalized cumulative frequencies plotted against the normalized instantaneous (frame to frame) velocities. This graph illustrates a very good agreement between the manual and automated tracking results which demonstrates the versatility and robustness of our cellular tracking algorithm when applied to challenging in-vivo data. The level of accuracy attained by our method allows a detailed analysis of biological implications associated with cellular migration.

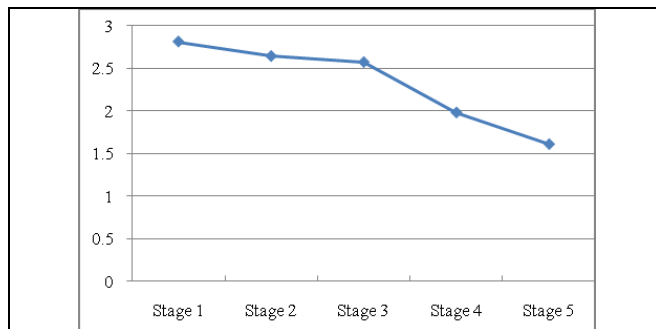


Fig. 4. Average normalized instantaneous cell velocities during different stages of the heart development.

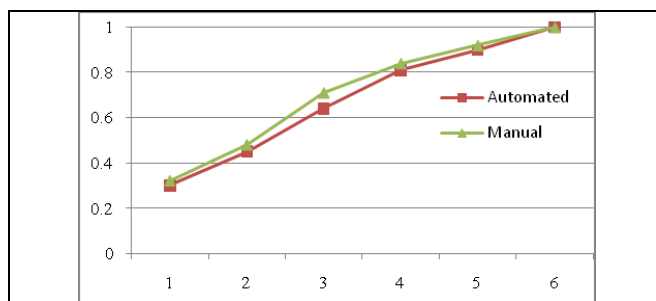


Fig. 5. Normalized instantaneous cell velocities versus normalized cumulative frequencies showing the amount of deviation between the cell velocities determined using the manually annotated data and automated *in-vivo* tracking.

## V. CONCLUSIONS

The proposed framework introduces a data-driven cellular tracking algorithm that does not require prior knowledge about the motion patterns or assumptions in regard to the image noise. The particles are independent and are able to adapt to local conditions, and as a result, the proposed framework is suitable to track the random motion of the cell nuclei. The performance attained by the proposed method when it has been applied to both 2D and 3D cellular data demonstrates robust tracking results that allow a detailed quantitative analysis of cell migration that helps in understanding the mechanism behind key biological processes.

## ACKNOWLEDGMENT

We would like to express our gratitude to Dr. Rusty Lansford (California Institute of Technology) for the transgenic quails, and Computational Imaging Group of Drs. Brenda Rongish and Charlie Little (University of Kansas Medical Center) for the transgenic image sequences.

## REFERENCES

- [1] O. Al-Kofahi, R. J. Radke, S. K. Goderie, Q. Shen, S. Temple and B. Roysam "Automated cell lineage construction: a rapid method to analyze clonal development established with Murine neural progenitor cells," *Cell Cycle*, vol. 5, no. 3, pp. 327-335, Feb. 2006.
- [2] A. Mosig, S. Jager, C. Wang, S. Nath, I. Ersoy, K. Palaniappan and S. Chen, "Tracking cells in life cell imaging videos using topological alignments," *Algorithms for Molecular Biology*, vol. 4:10, Jul. 2009.
- [3] F. Li, X. Zhou, J. Ma, and S. T. C. Wong "Multiple nuclei tracking using integer programming for quantitative cancer cell cycle analysis," *IEEE Trans. Medical Imaging*, vol. 29, pp. 96-105, Jan. 2010.
- [4] A. R. Horwitz, N. Watson, and J.T. Parsons, "Breaking barriers through collaboration: the example of the cell migration consortium," *Genome Biology*, vol. 3, no.11, pp. 2011.1-2011.4, 2002.
- [5] K. Thirusittampalam, M.J. Hossain, O. Ghita, P.F. Whelan, "A novel framework for tracking *in-vitro* cells in time-lapse phase contrast data, in *Proc. British Machine Vision Conference*, UK, 2010, pp. 69.1-69.11.
- [6] M. Dewan, M. Ahmad, and M Swamy, "Tracking biological cells in time-lapse microscopy: an adaptive technique combining motion and topological features", *IEEE Trans. Biomedical Engineering*, vo 58, no. 6, pp. 1637-1647, Jun. 2011.
- [7] M. S. Arulampalam, S. Maskell, N. Gordon, and T. Clapp, "A tutorial on particle filters for online nonlinear/non-Gaussian Bayesian tracking," *IEEE Trans. Signal Processing*, vol. 50, pp. 174-188, Feb. 2002.
- [8] Y Rui and Y. Chen, "Better proposal distributions: object tracking using unscented particle filter," in *Proc. 2001 IEEE Int. Conf. Computer Vision and Pattern Recognition*, vol. 2, pp. 786-793
- [9] K. Li, E.D. Miller, M. Chen, T. Kanade, L.E. Weiss and P.G. Campbell, "Cell population tracking and lineage construction with spatiotemporal context," *Medical Image Analysis*, vol. 12, pp. 546-566, 2008.
- [10] K Nummiaroa, E. Koller-Meierb, L. Gool, "An adaptive color-based particle filter", *Image and Vision Computing*, vol. 21, pp. 99-110, Jan. 2003.
- [11] E. Maggio and A. Cavallaro, "Hybrid particle filter and mean shift tracker with adaptive transition model", in *Proc. IEEE Int. Conf. Acoustics, Speech, and Signal Processing*, 2005, vol.2, pp. 221-224.
- [12] I. Smal, K. Draegestein, N. Galjart, W. Niessen, and E. Meijering, "Particle filtering for multiple object tracking in dynamic fluorescence microscopy images: application to microtubule growth analysis," *IEEE Trans. Medical Imaging*, vol. 27, no. 6, pp. 789-804, Jun. 2008
- [13] G. Rabut and J. Ellenberg, "Automatic real-time three-dimensional cell tracking by fluorescence microscopy," *J. Microscopy*, vol. 216, no. 2, pp. 131-137, Nov. 2004
- [14] J. Shi and C. Tomasi, "Good features to track", in *Proc. IEEE Int. Conf. Computer Vision and Pattern Recognition*, 1999, pp. 593-600.
- [15] B.D. Lucas and T. Kanade. "An iterative image registration technique with an application to stereo vision," in *Proc. Int. Joint Conf. Artificial Intelligence*, 1981, pp. 121-130
- [16] G. Hager, M. Dewan and C. Stewart, "Multiple kernel tracking with SSD," in *Proc. IEEE Conference on Computer Vision and Pattern Recognition*, 2004, vol. 1, pp. 790-797
- [17] M. J. Hossain, M. Dewan, A. Kiok and O. Chae, "A Linear Time Algorithm of Computing Hausdorff Distance for Content Based Image Analysis," *Circuits, Systems, and Signal Processing*, pp. 1-11. doi:10.1007/s00034-011-9284-y, March 2011.
- [18] Z. Khan, T. Balch, and F. Dellaert, "MCMC-based particle filtering for tracking a variable number of interacting targets," *IEEE Trans. Pattern Analysis and Machine Intelligence*, vol. 27, pp. 1805-1819, Nov. 2005.
- [19] Y. Sato, G. Poynter, D. Huss, M. B. Filla, A. Czirok, B. J. Rongish. C. D. Little, S. E. Fraser, and R. Lansford, "Dynamic analysis of vascular morphogenesis using transgenic quail embryos," *PLOS ONE*, vol. 5, no. 9, Sep. 2010.
- [20] A Czirok, P.A. Rupp, B.J. Rongish and C.D. Little, "Multi-field 3D scanning light microscopy of early embryogenesis." *J. Microscopy*. vol. 206, pp. 209-17, Jun. 2002.